Available online at www.sciencedirect.com

ScienceDirect

Journal of Membrane Science 285 (2006) 362–375

journal of MEMBRANE SCIENCE

www.elsevier.com/locate/memsci

Theoretical calculation on the membrane potential of charged porous membranes in 1-1, 1-2, 2-1 and 2-2 electrolyte solutions

Wei-Juan Shang, Xiao-Lin Wang*, Yang-Xin Yu

Department of Chemical Engineering, Tsinghua University, Beijing 100084, PR China

Received 21 June 2006; received in revised form 1 September 2006; accepted 5 September 2006
Available online 7 September 2006

Abstract

The space-charge (SC) model and the Teorell–Meyer–Sievers (TMS) model are widely employed to calculate the membrane potential of charged porous membranes in 1-1 electrolyte solutions, but few works with the other kinds of electrolyte solutions have been reported. In this article, membrane potentials for 1-1, 1-2, 2-1 and 2-2 electrolyte solutions have been calculated numerically based on the two models using parameters of concentration, pore radius and surface charge density. The results suggest that equivalent electrolyte concentration is more suitable to characterize the membrane potential in different kinds of electrolyte solutions than electrolyte concentration. Membrane potential approaches to the Nernst potential in the low concentration region, which indicates membrane potential in monovalent cation electrolyte solution is twice as large as that in divalent cation electrolyte solution. In the high concentration region, membrane potential is close to the diffusion potential, which implies membrane potential would be reversed if the diffusion coefficient ratio of coion and counterion is larger than 1.0. While in the intermediate concentration region, membrane potential as a function of electrolyte concentration is almost linear. In the comparison of the SC and TMS models, theoretical predictions by the two models for 1-2, 2-1 and 2-2 electrolyte solutions appear to be similar to those for 1-1 electrolyte solutions reported earlier by Westermann-Clark and Christoforou [3]. The two models coincide with each other when the radius, r_p, is less than 5.0 nm and the dimensionless charge density in the pore wall, q_0 is less than 1.0. Otherwise, the TMS model would overestimate the membrane potential. Furthermore, the membrane potential shows dependence on the ratio of the volume charge density to equivalent electrolyte concentration, ξ_f, q_0 and r_p by the SC model, but only varies with ξ_f irrespective of q_0 and r_p by the TMS model. These findings have a significant influence on the establishment of an appropriate theory to evaluate membrane potentials in different electrolyte solutions.

Keywords: Membrane potential; Space-charge model; Teorell–Meyer–Sievers model; Charged membranes

1. Introduction

In our previous paper [1], the nanofiltration membrane was selected as a representative charged porous membrane, which may consist of a bundle of cylindrical charged capillaries with the structural parameters (pore radius, r_p, and the ratio of membrane porosity to membrane thickness, $A_k/\Delta x$) and the electrical properties such as the surface charge density, q_w. Salt rejection and membrane parameters (the reflection coefficient, σ, and the solute permeability coefficient, ω) for 1-1 electrolyte solutions were numerically calculated by the space-charge (SC) model and the Teorell–Meyer–Sievers (TMS) model as a function of two-dimensionless parameters: the electrokinetic radius, r_p/λ_D, and the dimensionless potential gradient in the pore surfaces, q_0. The research reveals that the TMS model shows good agreement with the SC model in the calculation of salt rejection and membrane parameters if q_0 is less than 1.0 [1].

In the present study, we will focus on membrane potential that is defined as a potential difference arising between the solutions of an electrolyte with different concentrations at the constant temperature and pressure when they are separated by a uniform membrane with fixed ionizable groups [2]. At the interface between membrane and electrolyte solutions, the Donnan potential occurs due to the transfer of ions. Inside the membrane, the diffusion potential arises since ions would diffuse from the high concentration side to the low concentration side under a certain concentration gradient. Membrane potential is the summation of the Donnan potential and the diffusion potential, and it can be also named as the exclusion–diffusion potential [3]. Membrane

---

* Corresponding author. Tel.: +86 10 62794741; fax: +86 10 62794741.
E-mail addresses: shangwj03@mails.tsinghua.edu.cn (W.-J. Shang), xl-wang@tsinghua.edu.cn (X.-L. Wang), yangxyu@mail.tsinghua.edu.cn (Y.-X. Yu).

0376-7388/$ – see front matter © 2006 Elsevier B.V. All rights reserved.
doi:10.1016/j.memsci.2006.09.005

potential can be measured directly by determining the electrical properties of a membrane or the activities of ions inside the membrane. Also, it can be calculated by the TMS model and the SC model, respectively [2–7].

The earlier theoretical studies on membrane potential were almost based on the TMS model and developed by Kobatake and co-workers [2,4,5] and Lakshminarayanaiah and co-workers [6,7]. Kobatake and co-workers [2,4,5] derived an equation of membrane potential for uni-univalent electrolyte solutions and first proved that the derived equation agreed well with typical corresponding experimental data. Nikonenko et al. [8] investigated the influence of the 1-1 salt concentration, and the ratio of the diffusion boundary layers length and the counter-ions diffusion coefficient on the membrane potential of an ion-exchange membrane. The research work concluded that the membrane potential carried out numerically by the TMS model were similar to those obtained experimentally by Dammak if the salt concentration is less than 100 mol m^{-3}. Lefebvre et al. [9] derived the general equations of the membrane potential, and the filtration potential of a charged membrane in an arbitrary electrolyte solution using an analytical approach. The group has only limited their studies to the related aspects of the comparison of normalized filtration potential calculated numerically and analytically with no discussion on membrane potential [9]. The above analysis demonstrates that most studies of membrane potential evaluated by the TMS model have been emphasized with attention being given to the uni-univalent electrolytes. Nevertheless, there is not enough convincing theoretical investigation concerning the other kinds of electrolytes. It is worthwhile clarifying the fact whether the TMS model can be employed to evaluate membrane potential in multivalent electrolyte solutions.

The SC model, originally proposed by Osterle and co-workers [10–12], is a more realistic model to evaluate the membrane potential, since the SC model take into account the radical variation of ionic concentrations and electrical potential within cylindrical membrane capillaries. Over the past several decades, much work has been done with the algorithm and applications of the SC model in charactering membrane potential of the charged porous membrane. Osterle and co-workers [10–12] first adopted the series transformed methods to calculate the Poisson–Boltzmann equation. The membrane potential for 1-1 electrolyte solutions was studied, and the pioneer investigations revealed that the membrane potential approached to the Nernst potential when the Debye length was great enough. Ruckenstein and co-workers [13] employed a fourthe-order Runge-Kutta numerical method to investigate the membrane potentials for 1-1, 1-2, and 2-1 electrolyte solutions as a function of the salt concentration in the permeate side. The typical experiments verified the validity of the SC model were carried out by Westermann-Clark and co-workers [14,15] and the experiments were performed with aqueous solution of alkali chlorides and $MgCl_2$ in track-etched mica membranes. Meanwhile, some researchers endeavored to solve the Poisson–Boltzmann by approximate analytical methods, such as Wooding [16], Levine [17], Martinez [18], and so on. These studies conduced to the simplified calculation of the SC model. Subsequently, Rievet and co-workers [19–21] presented many electrokinetic and electrochemical properties of charged porous membrane in KCl, such as, the consistency of the properties from three different perspectives (streaming potential, membrane potential and electrolyte conductivity), the contributions of the electrokinetic and electrochemical behaviors for the separating layer to the global behaviors for the composite membranes and so on. Despite many fruitful works thrown light on the nature of the electrokinetic and electrochemical phenomena, there is not sufficient research work to expatiate various interesting phenomena of membrane potential in a symmetrical and dissymmetrical electrolyte solution by the SC model.

Regarding the comparison of the membrane potential calculated by the TMS model and the SC model, only a few studies have highlighted. Westermann-Clark and Christoforou once compared the results obtained by the two model for 1-1 electrolytes [3]. The authors showed that the two models gave similar results for low surface charge densities of pore wall, but for large surface charge densities, the results from the TMS model differed strongly from those of the SC model. The research work has contributed to understand the sources and implications of the agreements and the discrepancies in evaluating the membrane potential by the two models. However, the effect of electrovalence of different electrolytes on the membrane potential of charged membrane must be taken into account, so that a general appropriate theory to evaluate membrane potentials in different electrolytes could be established.

The purpose of this article is to extend the application of TMS model in estimating membrane potential for 1-1 electrolyte solutions to multivalent electrolyte solutions, and establish an applicable scope of the straightforward analytical TMS model through the comparison with the complex numerical SC model. The membrane potential suitable for an arbitrary electrolyte solution by the TMS model can be obtained according to the derivation of Lefebvre et al. [9]. During the calculation, we firstly introduce the Cardano formula to compute the Donnan equation analytically, which is more convenient and precise than the deduction method reported in the literature [9]. Concerning the SC model, we adopt the Runge–Kutta–Gill method to calculate Poisson–Boltzmann equation. Membrane potentials for 1-1, 1-2, 2-1, and 2-2 electrolyte solutions have been numerically calculated by the TMS model and SC model as a function of concentration and two-dimensionless parameters: the ratio of the volume charge density to salt concentration, ξ_f, and the electrokinetic radius, r_p/λ_D^f. The results estimated by the two models will be compared strictly. Finally, based on the comparison, the range where the two models coincide with each other will be provided.

2. Theory and calculation

2.1. Space-charge (SC) model

The space-charge model was originally proposed by Osterle and co-workers [10–12], and has been mainly applied to describe electrokinetic phenomena and transport characteristics of charged capillaries [13–23]. The basic equations of the SC model are the Poisson–Boltzmann equation for the radial distribution of electric potential and ion concentration, the Nernst–Planck equation for ion transport, and the Navier–Stokes equation for volumetric flow.

Wang et al. [1] followed the basic derivations used by Ruckenstein [13,24,25] and Smit [22,23], and presented the relationship of three flows and three relevant driving forces with the following phenomenological equations:

$$J_{\mathrm{V}} = \frac{r_{\mathrm{p}}^2}{8\mu}\left(-\frac{\mathrm{d}P_0}{\mathrm{d}x}\right) + \frac{r_{\mathrm{p}}^2 c\nu_1 K_{12}}{2\mu}\left(-RT\frac{\mathrm{d}\ln c}{\mathrm{d}x}\right) + \frac{RT\varepsilon_{\mathrm{r}}\varepsilon_0 K_{13}}{z_1 F\mu}\left(-\frac{\mathrm{d}\phi}{\mathrm{d}x}\right) \tag{1}$$

$$J_1 + J_2 = \frac{\nu_1 r_{\mathrm{p}}^2 c K_{21}}{8\mu}\left(-\frac{\mathrm{d}P_0}{\mathrm{d}x}\right) + \left[\frac{D_1\nu_1 c K'_{22}}{RT} + \frac{\nu_1^2 r_{\mathrm{p}}^2 c^2 K''_{22}}{2\mu}\right]\left(-RT\frac{\mathrm{d}\ln c}{\mathrm{d}x}\right) + \left[\frac{z_1\nu_1 D_1 F c K'_{23}}{RT} + \frac{\nu_1 RT\varepsilon_r\varepsilon_0 c K''_{23}}{z_1 F\mu}\right]\left(-\frac{\mathrm{d}\phi}{\mathrm{d}x}\right) \tag{2}$$

$$I = \frac{r_{\mathrm{p}}^2 z_1\nu_1 F c K_{31}}{8\mu}\left(-\frac{\mathrm{d}P_0}{\mathrm{d}x}\right) + \left[\frac{D_1 z_1\nu_1 F c K'_{32}}{RT} + \frac{z_1\nu_1^2 r_p^2 c^2 F K''_{32}}{2\mu}\right]\left(-RT\frac{\mathrm{d}\ln c}{\mathrm{d}x}\right) + \left[\frac{z_1^2\nu_1 D_1 F^2 c K'_{33}}{RT} + \frac{\nu_1 RT\varepsilon_r\varepsilon_0 c K''_{33}}{\mu}\right]\left(-\frac{\mathrm{d}\phi}{\mathrm{d}x}\right) \tag{3}$$

J_{V}, J_1+J_2 and I are the total volume flux, solute flux through a capillary and electric current, respectively. P_0 corresponds to effective pressure, $c(x)$ is the fictitious concentration inside the capillaries as mentioned by Sasidhar and Ruckenstein [13], ϕ is the axial component of total electrical potential, x denotes the axial direction of the capillary, and K_{ij} are the coefficients which are listed in Appendix A of our previous paper [1].

Introducing the dimensionless form and using the no electrical current condition, we can obtain the dimensionless expressions of three driving forces as follows [1]:

$$\frac{\mathrm{d}\bar{P}_0}{\mathrm{d}\bar{x}} = \frac{(\nu_1+\nu_2/\nu_1)J_{\mathrm{s}}^* L_3 - Pe\,\bar{c}L_1}{(L_2L_3 - L_1L_4)\bar{c}} \tag{4}$$

$$\frac{\mathrm{d}\bar{c}}{\mathrm{d}\bar{x}} = \frac{(\nu_1+\nu_2/\nu_1)J_{\mathrm{s}}^* L_4 - Pe\,\bar{c}L_2}{(L_2L_3 - L_1L_4)} \tag{5}$$

$$\frac{\mathrm{d}\bar{\phi}}{\mathrm{d}\bar{x}} = \frac{(\nu_1+\nu_2/\nu_1)J_{\mathrm{s}}^* L_6 - Pe\,\bar{c}L_5}{(L_2L_3 - L_1L_4)\bar{c}} \tag{6}$$

J_{s}^* and Pe are the dimensionless expressions of solute flux and the total volume flux through a capillary. $\bar{c}$ is the dimensionless concentration, ν_i are the stoichiometric coefficient of electrolyte, 1 represents counterion and 2 denotes co-ion. L_i are the coefficients listed in Appendix B of our previous paper [1]. Integrating the Eqs. of (4)–(6) from the high concentration side (c_{f}) to the low concentration side (c_{p}) through the membrane, one can obtain the following equations:

$$\Delta\bar{\phi}\big|_{\mathrm{SC}} = \int_1^{c_{\mathrm{p}}/c_{\mathrm{f}}} \frac{(\nu_1+\nu_2/\nu_1)(J_{\mathrm{S}}^*/Pe)L_6 - \bar{c}L_5}{(\nu_1+\nu_2/\nu_1)(J_{\mathrm{S}}^*/Pe)L_4 - \bar{c}L_2}\frac{\mathrm{d}\bar{c}}{\bar{c}} \tag{7}$$

$$\Delta\bar{P}_0 = Pe_{\mathrm{p}} - Pe_{\pi} = \int_1^{c_{\mathrm{p}}/c_{\mathrm{f}}} \frac{(\nu_1+\nu_2/\nu_1)(J_{\mathrm{S}}^*/Pe)L_3 - \bar{c}L_1}{(\nu_1+\nu_2/\nu_1)(J_{\mathrm{S}}^*/Pe)L_4 - \bar{c}L_2}\frac{\mathrm{d}\bar{c}}{\bar{c}} \tag{8}$$

where

$$Pe_{\mathrm{p}} = \frac{r_{\mathrm{p}}^2(P_1 - P_2)}{8\mu D_1} \tag{9}$$

$$Pe_{\pi} = \frac{RTr_{\mathrm{p}}^2(\nu_1+\nu_2)(c_1 - c_2)}{8\mu D_1} = \frac{r_{\mathrm{p}}^2\Delta\pi}{8\mu D_1} \tag{10}$$

$\Delta\bar{\phi}_{\mathrm{SC}}$ is the dimensionless membrane potential and $\Delta\bar{P}_0$ is the dimensionless effective pressure. Pe_{p} represents the Peclet number for the Poiseuille flow velocity computed at the applied pressure drop, whereas Pe_{π} represents the Peclet number for the osmotically driven flow in an ideal semipermeable membrane.

The scheme is as follows. The Poisson–Boltzmann equation is first solved for different values of $c(c_{\mathrm{f}} \geq c \geq c_{\mathrm{p}})$. Hence, the values of the coefficients K_{ij} and L_i can be calculated for various values of the argument $\bar{c}$. Then, a value is chosen for the ratio J_{S}^*/Pe and the integral in Eq. (8) is evaluated to obtain a value of Pe_{p}. The ratio J_{S}^*/Pe is varied until the computed value of Pe_{p} matches the originally specified value ($Pe_{\mathrm{p}} = 0$ for osmotically driven flows). Once the ratio J_{S}^*/Pe for a specified Pe_{p} is acquired, the integral of Eq. (7) is evaluated to obtain the corresponding value of $\Delta\bar{\phi}_{\mathrm{SC}}$. The algorithm adopted here is equivalent to the approach reported in the pertinent literature [3].

2.2. *Teorell–Meyer–Sievers (TMS) model*

The Teorell–Meyer–Sievers model was originally proposed by Teorell, Meyer and Sievers [26,27], and has been applied to describe transport characteristics and electrokinetic phenomena of charged capillaries [2–9,28–33]. The basic equations of the TMS model are the Donnan equation for the partition coefficients of ion concentrations at the surface between the membrane and the external solution, the Nernst–Planck equation, and the different electroneutrality conditions for the inside membrane and the external solutions.

According to the derivation of Lefebvre and co-workers [9,33], the dimensionless membrane potential can be expressed

$$\Delta\bar{\phi}_{\mathrm{TMS}} = \frac{1}{z_2}\ln\frac{k_2^{\mathrm{p}}}{k_2^{\mathrm{f}}} + \frac{D_1 - D_2}{z_2D_2 - z_1D_1}\ln\left(\frac{T_{\mathrm{r}}k_2^{\mathrm{p}} + t_1\xi_{\mathrm{f}}}{k_2^{\mathrm{f}} + t_1\xi_{\mathrm{f}}}\right) \tag{11}$$

where

$$\Delta\bar{\phi} = \frac{F\Delta\phi}{R_gT}, \quad t_1 = \frac{|z_1|D_1}{|z_1|D_1 + |z_2|D_2},$$

$$\xi_f = \frac{|X_m|}{|z_1|\upsilon_1 c_f}, \quad T_r = \frac{c_p}{c_f}$$

z_i, D_i and k_i are the electrochemical valence, diffusion coefficient and partition coefficient of ion i. T_r is the transmission, which denotes the ability of solute to pass through the membrane. $\xi_{f(p)}$ is the ratio of the volume charge density to equivalent salt concentration in the feed side or in the permeate side of membrane. F is the Faraday constant, R_g is the gas constant and T is the temperature. $\Delta\bar{\phi}$ represents the dimensionless form of the membrane potential, $\Delta\phi$. X_m is the constant volume charge density of charged membrane (mole/l of pore volume).

The membrane is assumed to be a positively charged membrane. Concerning the 1-1 electrolyte, the partition coefficient of co-ion is expressed as follows:

$$k_2^{p(f)} = \frac{-\xi_{p(f)} + \sqrt{\xi_{p(f)}^2 + 4}}{2}, \quad \xi_{p(f)} = \frac{-X_m}{z_1\upsilon_1 c_{p(f)}} \tag{12}$$

By combining the Eqs. of (11) and (12), membrane potential can be obtained in another version

$$\Delta\bar{\phi}_{\mathrm{TMS},1:1} = -\ln\frac{\xi_f}{\xi_p}\frac{1+\sqrt{1+4/\xi_f^2}}{1+\sqrt{1+4/\xi_p^2}} - W\ln\left(\frac{\sqrt{1+4/\xi_p^2}+W}{\sqrt{1+4/\xi_f^2}+W}\right), \quad W = \frac{D_1 - D_2}{D_1 + D_2} \tag{13}$$

The Eq. of (13) is a well-known expression predicting the dimensionless membrane potential for 1-1 electrolyte by the TMS model [2–5,34–36]. It is noted that the dimensionless membrane potential is caused only by the concentration differences with no volumetric flux condition. That is, the contribution of the osmotic pressure to the volumetric flux is negligible. Therefore, it may be applicable for very narrow pore or very low concentrations.

Regarding other symmetric electrolytes ([z:z]), the expressions of the ionic partition coefficient and dimensionless membrane potentials are the same as 1-1 electrolyte [9,33].

As to 1-2 asymmetric salt, the partition coefficient of co-ion can be expressed as follows [9,33]

$$k_2^{p(f)} = [\Gamma_{1:2,p(f)}^-]^{-2},$$

$$\Gamma_{1:2,p(f)}^- = \left[\frac{\Lambda(1,1,\xi_{p(f)})^{1/3}}{6} - \frac{2\xi_{p(f)}}{\Lambda(1,1,\xi_{p(f)})^{1/3}}\right]^{-1} \tag{14}$$

where

$$\Lambda(1,1,\xi_{p(f)}) = 108 + 12\sqrt{3}\sqrt{(27 + 4\xi_{p(f)}^3)}$$

As far as a 2-1 asymmetric salt is concerned, the expression of the partition coefficient of co-ion is more complicated. When $27 - 4\xi_{p(f)}^3$ is larger than zero, the expression of the ionic partition coefficient of a 2-1 asymmetric salt is similar to that of a 1-2 asymmetric salt [9,33]

$$k_2^{p(f)} = [\Gamma_{2:1,p(f)}^-]^{-1}$$

$$\Gamma_{2:1,p(f)}^- = \frac{\Lambda(1,1,-\xi_{p(f)})^{1/3}}{6} + \frac{2\xi_{p(f)}}{\Lambda(1,1,-\xi_{p(f)})^{1/3}} \tag{15}$$

where

$$\Lambda(1,1,-\xi_{p(f)}) = 108 + 12\sqrt{3}\sqrt{(27 - 4\xi_{p(f)}^3)}$$

When $27 - 4\xi_{p(f)}^3$ is less than zero, the Eq. of (15) is inapplicable. Fortunately, Cardano formula is powerful enough to deal with the situation. According to the Cardano formula, there are three roots for normal cubic equation with one argument unknown as $x^3 + px + q = 0$ [37]

$$x_1 = \sqrt[3]{-\frac{q}{2}+\sqrt{\Delta}} + \sqrt[3]{-\frac{q}{2}-\sqrt{\Delta}};$$

$$x_2 = \omega\sqrt[3]{-\frac{q}{2}+\sqrt{\Delta}} + \omega^2\sqrt[3]{-\frac{q}{2}-\sqrt{\Delta}};$$

$$x_3 = \omega^2\sqrt[3]{-\frac{q}{2}+\sqrt{\Delta}} + \omega\sqrt[3]{-\frac{q}{2}-\sqrt{\Delta}} \tag{16}$$

where

$$\Delta = \left(\frac{q}{2}\right)^2 + \left(\frac{p}{3}\right)^3, \quad \omega = \frac{-1+\sqrt{3}i}{2} = \cos\frac{2\pi}{3} + i\sin\frac{2\pi}{3},$$

$$\omega^2 = \frac{-1-\sqrt{3}i}{2} = \cos\frac{4\pi}{3} + i\sin\frac{4\pi}{3}$$

If $\Delta > 0$, the normal cubic equation has only one real root, x_1, and two imaginary roots, x_2, x_3. If $\Delta > 0$, the normal cubic equation have three real roots, x_1, x_2, x_3, represented as follows:

$$x_1 = 2\sqrt[3]{-\frac{q}{2}}; \qquad x_2 = x_3 = -\sqrt[3]{-\frac{q}{2}} \tag{17}$$

If $\Delta < 0$, x_1, x_2, x_3, are all real roots to normal cubic equation

$$x_1 = \sqrt[3]{\rho}\,e^{i\theta/3} + \sqrt[3]{\rho}\,e^{-i\theta/3} = 2\sqrt[3]{\rho}\cos\frac{\theta}{3} = 2\sqrt{-\frac{p}{3}}\cos\frac{\theta}{3};$$

$$x_2 = 2\sqrt[3]{\rho}\cos\frac{\theta+2\pi}{3} = 2\sqrt{-\frac{p}{3}}\cos\frac{\theta+2\pi}{3};$$

$$x_3 = 2\sqrt[3]{\rho}\cos\frac{\theta+4\pi}{3} = 2\sqrt{-\frac{p}{3}}\cos\frac{\theta+4\pi}{3} \tag{18}$$

where

$$\rho = \sqrt{\left(-\frac{q}{2}\right)^2 + (\sqrt{-\Delta})^2} = \sqrt{\left(-\frac{p}{3}\right)^3},$$

$$\cos\theta = \frac{-q/2}{\rho}, \left(0 < \theta < \frac{\pi}{2}\right) \tag{19}$$

From the Eqs. of (17) and (19), it is easy to verify $x_1 > 0$, $x_2 < 0$, $x_3 < 0$. In practice, x_1 is the right root.

Utilizing the above-mentioned Cardano formula, one can easily obtain the ionic partition coefficients of 1-2 and 2-1 asymmetric electrolyte solutions and solve the problem existed in the Eq. of (15). When $27-4\xi^3_{\text{p(f)}}$ is less than zero, the partition coefficient of co-ion in a 2-1 asymmetric salt is expressed as follows:

$$k_2^{\text{p(f)}} = [\Gamma^{-}_{2:1,\text{p(f)}}]^{-1}, \quad \Gamma^{-}_{2:1,\text{p(f)}} = 2\sqrt{\frac{\xi_{\text{p(f)}}}{3}}\cos\frac{\theta}{3},$$

$$\theta = \arccos\left(\frac{1}{2}\left(\frac{\xi_{\text{p(f)}}}{3}\right)^{-1.5}\right) \tag{20}$$

The scheme is as follows. The partition coefficient of co-ion is first solved for different values of c_f and with the concentration ratio c_f/c_p constant through the Cardano formula introduced in this article. Then, $\Delta\bar{\phi}_{\text{TMS}}$ can be obtained according to the Eq. of (11) for various values of c_f.

3. Results and discussion

3.1. The effect of the electrovalence, concentration ratio, c_f/c_p, and diffusion coefficients ratio, D_2/D_1, of an electrolyte solution on the membrane potential

3.1.1. The influence of the ion valence on the membrane potential

The dimensionless membrane potential, $\Delta\bar{\phi}$, of the eight salt solutions was obtained by the SC model and TMS model under the conditions that negatively charged porous membranes with the pore radius r_p of 5.0 nm and the surface charge density q_w of $-6.672\times10^{-3}\,\text{C}\,\text{m}^{-2}$. The pore radius employed here is according to the interesting features on molecular weight cut-off (MWCO) of charged porous membrane [1]. In accordance with the Stokes–Einstein relationship, the pore diameters suitable for electrolyte solutions range from 1 to several nm. In our study, we choose 5.0 nm as a representative pore radius to study the influence of different electrolyte solutions since the impact of pore radius on membrane potential are discussed in the following aspect. In terms of the surface charge density, many studies suggest that the magnitude is about $10^3\,\text{esu}\,\text{cm}^{-2}$ [13,14]. Moreover, the value of $10^3\,\text{esu}\,\text{cm}^{-2}$ is equal to $3.336\times10^{-3}\,\text{C}\,\text{m}^{-2}$ in the standard unit. To survey the effect of different electrolyte solutions, we choose 2.0 times of the magnitude of $10^3\,\text{esu}\,\text{cm}^{-2}$ as a typical surface charge density since the impact of surface charge density on membrane potential are discussed as another separate aspect. The eight salts are KCl, NaCl, K_2SO_4, Na_2SO_4, $MgCl_2$ and $CaCl_2$, $MgSO_4$ and $CaSO_4$ with the concentration from 1.0 to 1000.0 mol m^{-3}. The relationship of the surface charge density, q_w and the volume charge density, X_m is $X_\text{m} = 2q_\text{w}/Fr_\text{p}$, where F is the Faraday constant.

As shown in Fig. 1, $\Delta\bar{\phi}$ calculated by the two models tend to coincide with each other. It is indicated that $\Delta\bar{\phi}$ approaches to some certain values in the low- and high-concentration regime. In the low-concentration range, the co-ions are almost completely excluded from the pores due to the high double-layer repulsion, and the distribution of ions arising by the diffusion of counterion is the main reason to the membrane potential [13]. Under such circumstances, the diffusion effect can be ignored, and the membrane potential is mainly dominated by the Donnan effect. Assuming the ideal circumstances, $\mu_1^\text{f} \approx \mu_1(0^+)$, and $\mu_1^\text{p} \approx \mu_1(l_m^-)$. According to $\mu_1^\text{f} - \mu_1(0^+) = \mu_1^\text{p} - \mu_1(l_m^-)$ and the expressions of $\mu_1^{\text{f(p)}}$ [9], one can get

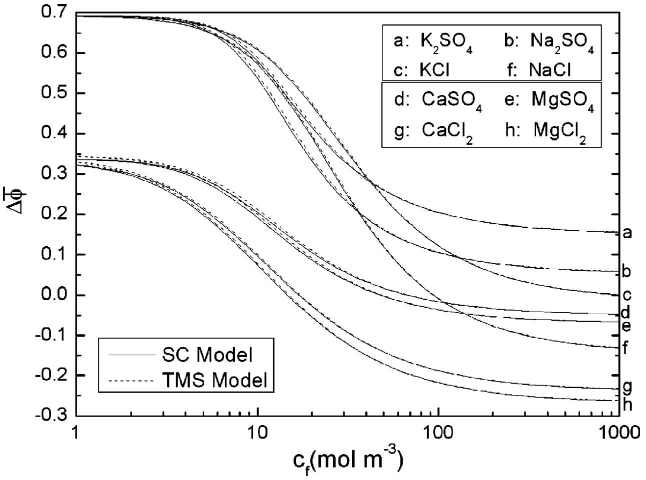

Fig. 1. $\Delta\bar{\phi}$ as a function of c_f for eight electrolyte solutions (NaCl; KCl; Na_2SO_4; K_2SO_4; $MgCl_2$; $CaCl_2$; $MgSO_4$; $CaSO_4$) under the condition that c_f/c_p is 2.0, r_p is 5.0 nm, and q_w is $-6.672\times10^{-3}\,\text{C}\,\text{m}^{-2}$.

$$RT\ln c_1^\text{f} - z_1F\Delta\phi^\text{f} = RT\ln c_1^\text{p} - z_1F\Delta\phi^\text{p}$$

$$\Delta\bar{\phi} \cong -\Delta\bar{\phi}^\text{p} + \Delta\bar{\phi}^\text{f} = \frac{1}{z_1}\ln\left(\frac{c_\text{f}}{c_\text{p}}\right) \tag{21}$$

$c_1^{\text{f(p)}}$ represent the counter-ion concentrations in the feed side and the permeate side. The Eq. of (21) states that membrane potentials approaches to the Nernst potential at very low concentrations. That is, the membrane potential corresponds to the electrovalences of counter-ions and the ratio of solute concentrations in both sides of charged porous membranes. If the electrovalence of counter-ions is doubled without changing the other conditions, the membrane potential becomes only one-half less. It is clear that the membrane performance closely approaches that of an ideal semipermeable membrane (zero solute permeability).

On the other hand, in the high-concentration range, the electrical double layers formed in the pore are compressed and hence almost the entire pore volume is electrically neutral [13]. Thus, the Donnan effect can be neglected. Under the ideal condition, $\xi_\text{f} = |X_m|/|z_1|\nu_1 c_{\text{f(p)}} \cong 0$, and the dimensionless membrane potential is nothing but the free diffusion potential given by [9]

$$\Delta\bar{\phi} \cong \Delta\bar{\phi}^\text{d} = \frac{D_2 - D_1}{z_2D_2 - z_1D_1}\ln\left(\frac{c_\text{f}}{c_\text{p}}\right) \tag{22}$$

The Eq. of (22) implies that the membrane potential closes to the diffusion potential at high concentrations. That is, the membrane potential is a function of ionic diffusion coefficients, ionic electrovalences and the ratio of solute concentrations in both sides of charged porous membranes.

In the intermediate-concentration regime, neither the Donnan effect nor the diffusion effect can be negligible. As a result, the values of membrane potentials, between the above two limits, increase as the concentrations of the electrolytes becomes lower. As to two different kinds of electrolytes with the membrane potentials between the same Donnan potential and different diffusion potentials, such as KCl and K_2SO_4, NaCl and Na_2SO_4, their dimensionless membrane potentials have a crossover in intermediate-concentration regime. The crossover phenomena can be explained by the electrovalence of ions.

As shown in Fig. 2, the crossover phenomena disappears when the argument of the salt concentration is multiplied with $z_i \nu_i$. That is, the membrane potential as a function of electrolyte concentration is redesigned by the membrane potential as a function of equivalent electrolyte concentration. The crossover phenomenon may be also disappears when the other parameters (ion rejection rate, the partition coefficient of ions and so on) calculated by the two models is represented as a function of equivalent electrolyte concentration. Concerning the other two different kinds of electrolytes, $MgCl_2$ and $MgSO_4$, $CaCl_2$ and $CaSO_4$, there are no crossover phenomena whether the variable is the concentration or the equivalent concentration. The reason is that the products of $z_i \nu_i$ for 2-1 and 2-2 electrolyte are equal. The relationship between the membrane potential and the concentration is only a valid compressed

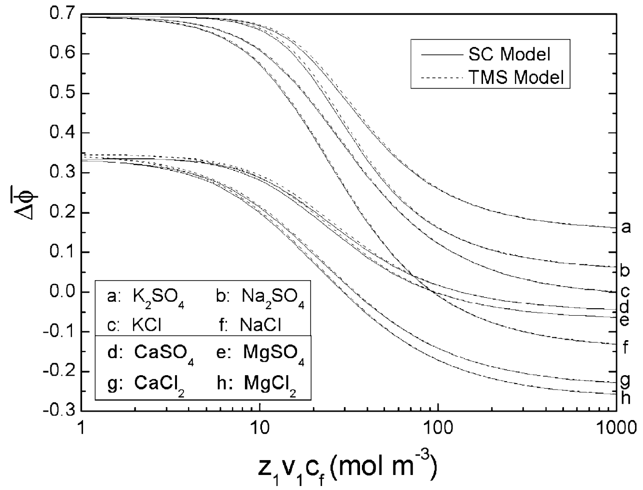

Fig. 2. $\Delta\bar{\phi}$ as a function of $z_1 \nu_1 c_f$ for eight electrolyte solutions (NaCl; KCl; Na_2SO_4; K_2SO_4; $MgCl_2$; $CaCl_2$; $MgSO_4$; $CaSO_4$) under the condition that c_f/c_p is 2.0, r_p is 5.0 nm, and q_w is -6.672×10^{-3} C m^{-2}.

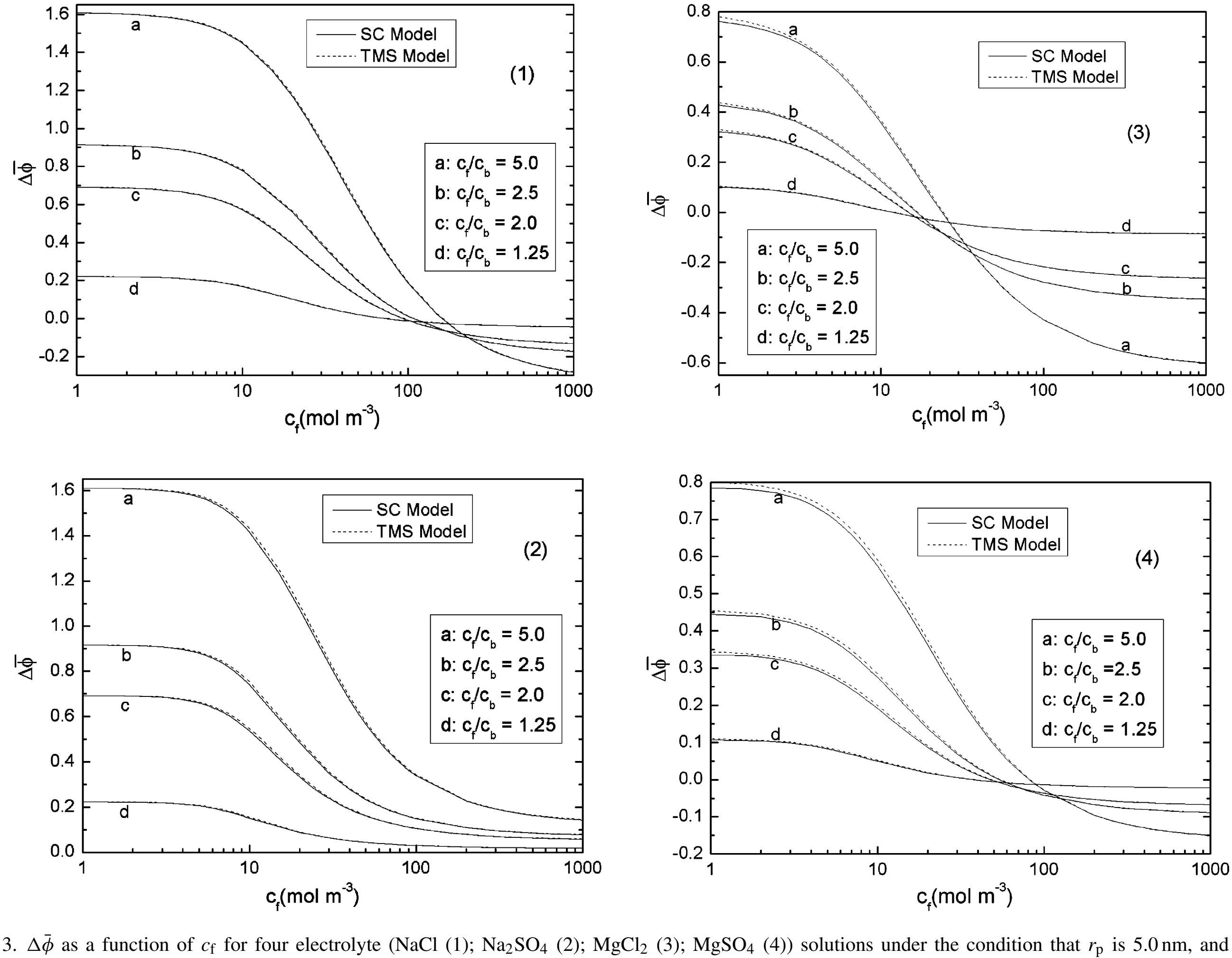

Fig. 3. $\Delta\bar{\phi}$ as a function of c_f for four electrolyte (NaCl (1); Na_2SO_4 (2); $MgCl_2$ (3); $MgSO_4$ (4)) solutions under the condition that r_p is 5.0 nm, and q_w is -6.672×10^{-3} C m^{-2}, and c_f/c_p is from 1.25 to 5.0.

approximation to the exact connection between the membrane potential and the equivalent concentration. Therefore, the employment of equivalent electrolyte concentration is favorable to investigate the membrane potential of different kinds of electrolytes.

Besides, the correlative interesting thing indicated by Fig. 2 is that ionic strength is also beneficial to study membrane potential. Ionic strength is a common quantity as half of the summary of ionic concentration multiplied by ionic electrovalence squared. If I is employed to describe ionic strength, it can be expressed, $I = 1/2\sum_i z_i^2 c_i$. c_i here is the concentration of ion i in mole/kg, which is approximate to the concentration of ion i in mole/l. According to the electroneutrality condition, $z_1c_1 + z_2c_2 = 0$, one can get another version of ionic strength, $I = 1/2(z_1 - z_2)z_1c_1 = 1/2(z_1 - z_2)z_1\nu_1c_s$. Where c_s is the concentration of salt solution. The difference between ionic strength, I, and equivalent electrolyte concentration, $z_1\nu_1c_s$, is the expression of $1/2(z_1 - z_2)$. When the argument of equivalent electrolyte concentration is multiplied by $1/2(z_1 - z_2)$, the horizontal axis will reduce to 1.0, 1.5, 1.5, and 2.0 times for 1-1, 1-2, 2-1 and 2-2 electrolyte solutions, respectively. Moreover, the variation is beneficial to eliminate the crossover phenomena. In other words, ionic strength is favorable for membrane potential as well as equivalent electrolyte concentration.

3.1.2. The influence of the concentration ratio (c_f/c_p) on the membrane potential

Fig. 3 presents $\Delta\bar{\phi}$ as a function of c_f for four electrolyte (NaCl(1); Na_2SO_4(2); $MgCl_2$(3); $MgSO_4$(4)) solutions at the radius r_p of 5.0 nm, the surface charge density q_w of $-6.672 \times 10^{-3}\,C\,m^{-2}$ and the concentration ratio c_f/c_p from 1.25 to 5.0. It should be noted that the selection of c_f/c_p as 5:1, 5:2, 2:1 and 5:4 is due to the widely application of binary logarithm and decimal logarithm.

As shown in the figure, $\Delta\bar{\phi}$ for different electrolyte systems vary differently with the concentration ratio. As far as Na_2SO_4 is concerned, $\Delta\bar{\phi}$ decreases with the decrease of the concentration ratio monotonely. While for the other three electrolyte, $\Delta\bar{\phi}$ firstly decreases as the concentration ratio decreases in the low-concentration region, but then increases as the concentration ratio decreases in the high-concentration region. The differences can be explained from Eq. of (21), valid at low feed concentration, and (22), valid at high feed concentration. The Eq. of (21) can predict the same order of $\Delta\bar{\phi}$

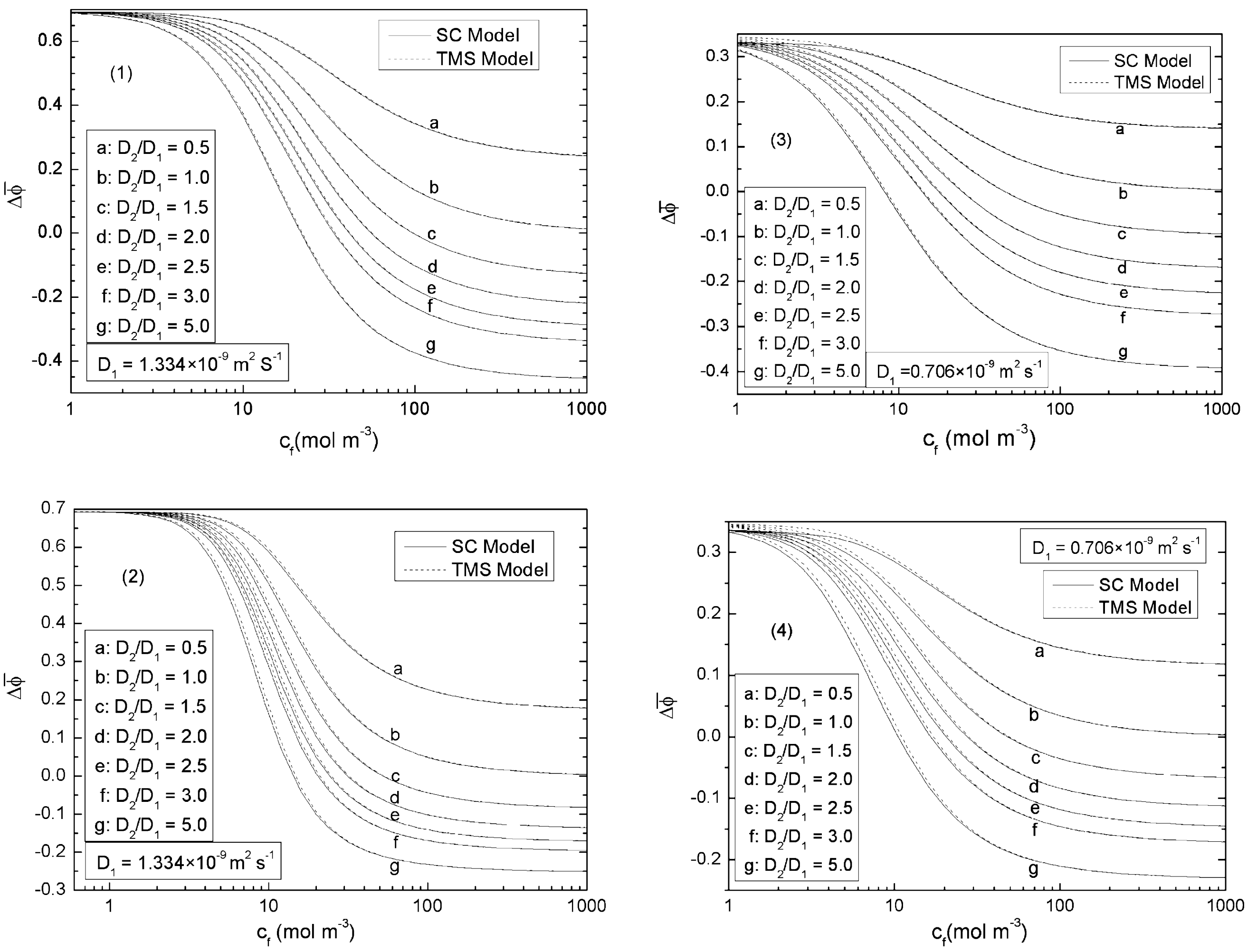

Fig. 4. $\Delta\bar{\phi}$ as a function of c_f for four fictitious electrolyte (1-1 (1); 1-2 (2); 2-1 (3); 2-2 (4)) solutions under the condition that c_f/c_p is 2.0, r_p is 5.0 nm, and q_w is $-6.672 \times 10^{-3}\,C\,m^{-2}$.

as a function of the concentration ratio as the figure provided. The Eq. of (22) can be written as

$$\Delta\bar{\phi} \cong \Delta\bar{\phi}^{\mathrm{d}} = \frac{D_2/D_1 - 1.0}{z_2 D_2/D_1 - z_1} \ln\left(\frac{c_{\mathrm{f}}}{c_{\mathrm{p}}}\right) \tag{23}$$

The relation reflected by the Eq. of (23) clearly shows that the order of membrane potentials as a function of the concentration ratio is inverted depending on whether the diffusion coefficients ratio, D_2/D_1 is less or more than 1.0. Consequently, the diffusion coefficients ratio is only source of the differences.

In the intermediate-concentration regime, Figs. 3 and 4 indicate that the membrane potential as a function of electrolyte concentration is almost linearity. This relationship can also be found in some experiment work [2–5,38,39].

3.1.3. The influence of the diffusion coefficients ratio (D_2/D_1) on the membrane potential

To clarify the effect of the diffusion behaviors to the membrane potential farther, fictitious electrolytes are introduced, which are composed of suppositional ions with different valence and diffusion coefficient. Fig. 4 describe $\Delta\bar{\phi}$ as a function of c_{f} for four fictitious electrolyte (1-1(1); 1-2(2); 2-1(3); 2-2(4)) solutions at the radius r_{p} of 5.0 nm, the surface charge density q_{w} of -6.672×10^{-3} C m^{-2} and the concentration ratio $c_{\mathrm{f}}/c_{\mathrm{p}}$ of 2.0. The diffusion coefficients ratio, D_2/D_1, is chose in the range of 0.5–5.0. The selection is based on the commonly known ionic diffusion coefficients. Generally, counter-ionic diffusion coefficient varies between 0.5 and 2.0 except H$^+$, while co-ionic diffusion coefficients change from 1.0 to 2.5 except OH$^-$. Thus, membrane potential is calculated under the condition that the values of D_2/D_1 vary between 0.5 and 5.0.

From the figure, $\Delta\bar{\phi}$ decreases with the increase of D_2/D_1 for the same electrolyte. When D_2/D_1 more than 1.0, the membrane potential would be reversed, in the high concentration region compared with those in the low concentration region without reference to the electrovalence of an electrolyte. Furthermore, the concentration resulted in the reversed membrane potential decrease with the increase of D_2/D_1. Take the ratios of diffusion coefficients up to 5.0 for an instance, the concentration is less than 25.0 mol m^{-3} for four fictitious electrolyte (1-1(1); 1-2(2); 2-1(3); 2-2(4)) solutions. The reversed behaviors can be interpreted form the Eq. of (23) effortlessly. However, the more interesting thing implied by the figure is that ionic mobilities or even the rejection change greatly. Since the diffusion coefficients

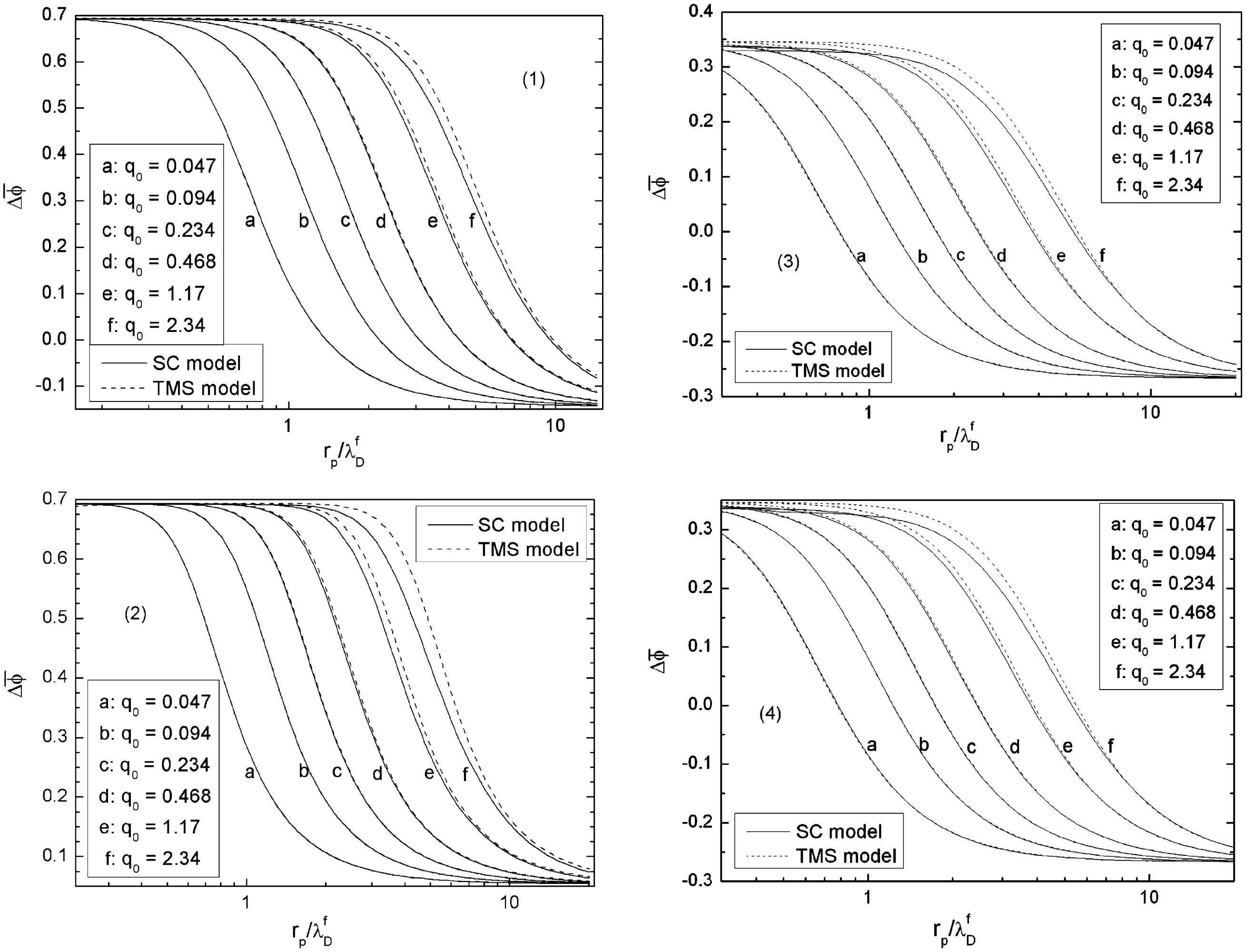

Fig. 5. $\Delta\bar{\phi}$ as a function of $r_{\mathrm{p}}/\lambda_{\mathrm{D}}^{\mathrm{f}}$, and q_0 for four electrolyte (NaCl (1); Na$_2$SO$_4$ (2); MgCl$_2$ (3); MgSO$_4$ (4)) solutions under the condition that $c_{\mathrm{f}}/c_{\mathrm{p}}$ is 2.0, r_{p} is 5.0 nm, and q_0 is from 0.047 to 2.34.

are independent of the Donnan potential, the reversed membrane potential is determined by the diffusion potential. According to the dimensionless diffusion potential in the membrane reported earlier [7], it can be expressed

$$\Delta\bar{\phi} = \left(\frac{\text{ts}_1}{z_1} - \frac{\text{ts}_2}{z_2}\right) \ln\left(\frac{c_\text{f}}{c_\text{p}}\right) \tag{24}$$

ts_i represents ionic transport rate. The Eq. of (24) reveals that the mobilities of counter-ion and co-ion will intersect before the membrane potential is equal to zero if D_2/D_1 is greater than 1.0. That is, when compared a positive membrane potential with a negative membrane potential at the same concentration of different electrolytes, such as curve a and curve f for 1-1 fictitious electrolyte, the mobilities of counter-ion and co-ion have a crossover for the electrolyte with the negative membrane potential, but have no crossover for the electrolyte with the positive membrane potential. The transformation of ionic mobilities may again influence electrolyte transport properties, and the rejection of membrane to ions may also changed from great to small, or even become minus at certain concentration region. Thus, the diffusion coefficients ratio is an important parameter on the prediction and interpretation of electrolyte electrical and transport properties.

Besides, when the counter-ion and the ratio of the diffusion coefficients ratio, D_2/D_1, is the same, the membrane potential decreases with the increasing of co-ion valence. It can also be interpreted form the Eq. of (23) without needing much effort.

From the above study of the impact of the electrovalence, concentration ratio, c_f/c_p, and diffusion coefficients ratio, D_2/D_1, of an electrolyte solution on the membrane potential, one can reach another conclusion that simple analytical TMS model can predict membrane potential for 1-1, 1-2, 2-1, and 2-2 electrolyte solutions perfectly as well as the complex numerical SC model. Moreover, various anomalous phenomena can be explained expediently by the TMS model when compared with the SC model. The possible reason is that the linearized transport equations (Eqs. of (1)–(3)) are difficult to analyze due to the concentration gradient and the concentration dependence of the coupling coefficients (K_{ij}) [3].

3.2. Membrane potential as a function of two-dimensionless parameters: ξ_f, r_p/λ_D^f under various r_p and q_0 of charged porous membranes

In this part, the dimensionless membrane potential, $\Delta\bar{\phi}$, was calculated by the SC model and TMS model as a function of

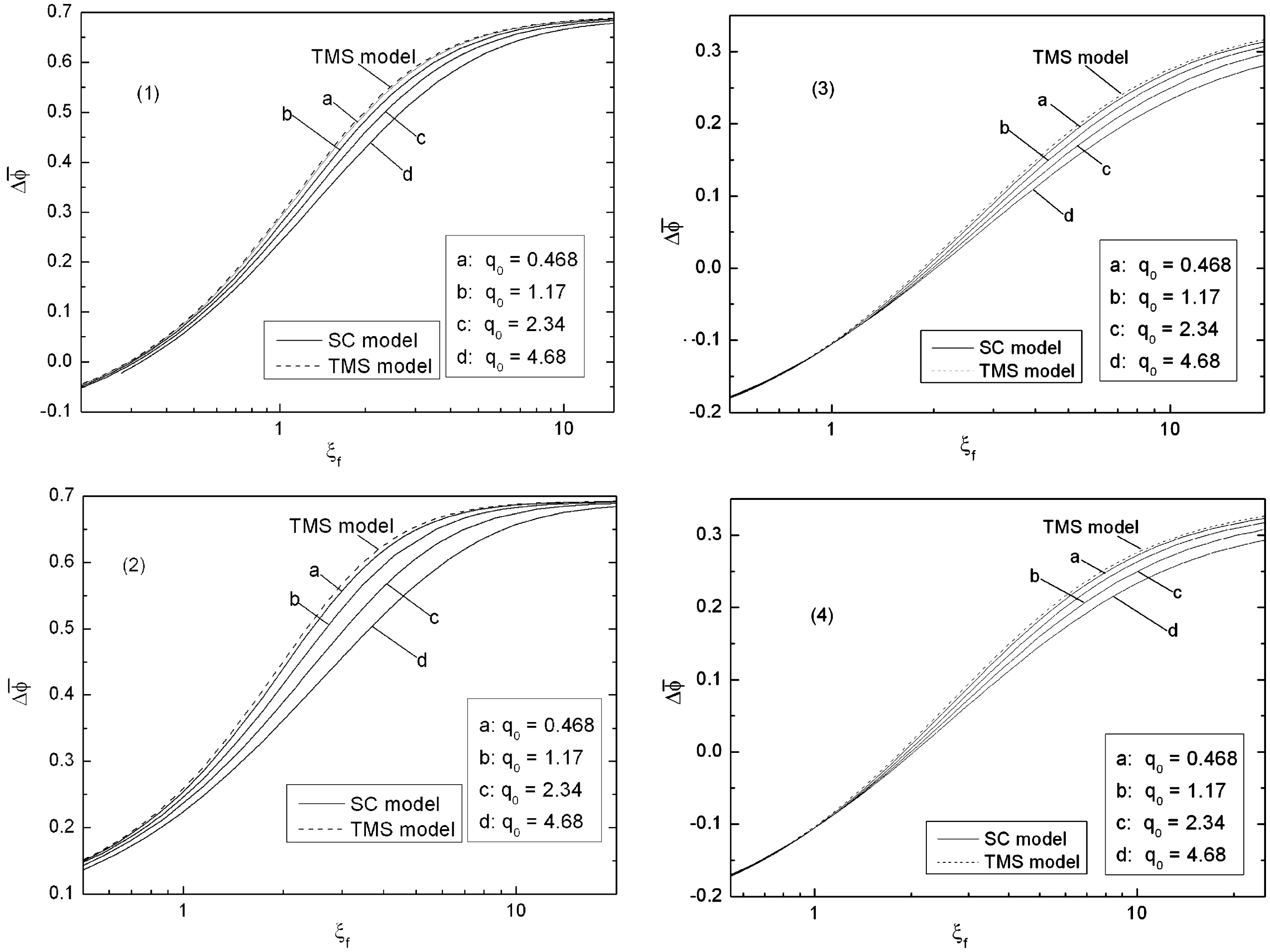

Fig. 6. $\Delta\bar{\phi}$ as a function of ξ_f, and q_0 for four electrolyte (NaCl (1); Na_2SO_4 (2); $MgCl_2$ (3); $MgSO_4$ (4)) solutions under the condition that c_f/c_p is 2.0, r_p is 5.0 nm, and q_0 is from 0.468 to 4.68.

three-dimensionless parameters: the ratio of the volume charge density to the salt concentration on the feed side, ξ_f, the electrokinetic radius, r_p/λ_D^f and the dimensionless charge density in the pore wall, q_0. As mentioned in our previous paper [1], the effect of equivalent concentration at the feed side can be expressed by the Debye length, $\lambda_D^f = [2\nu_1 z_1 F^2 c_f / R_g T \varepsilon_r \varepsilon_0]^{-0.5}$, since $1/\lambda_D^f$ is proportional to $[\nu_1 z_1 c_f]^{0.5}$. F is the Faraday constant, R_g is the ideal gas constant, and T is the tempeture (K). The dimensionless parameter q_0 is comprised of the surface charge density, q_w, and the pore radius, r_p, in the form of their products, $q_0 = Fr_p|q_w|/(4\varepsilon_r\varepsilon_0 RT)$. While the dimensionless parameter ξ_f is the ratio of the constant membrane charge density (mole/l of pore volume) and ion concentration, $\xi_f = |X_m|/|z_1|\nu_1 c_f = 16q_0/(r_p/\lambda_D^f)^2$. The calculation was carried out under the conditions that negatively charged porous membranes for four salt solutions (NaCl, Na_2SO_4, $MgCl_2$ and $MgSO_4$) with the concentration from 1.0 to 1000.0 mol m^{-3}. As shown before, the pore diameters suitable for electrolyte solutions range from 1 to several nm and the magnitude is about 10^3 esu cm^{-2}, that is, 3.336×10^{-3} C m^{-2} in the international unit. In this section, we choose r_p in the range of 1.0–20.0 nm and q_w from -6.672×10^{-4} to -6.672×10^{-2} C m^{-2} to investigate membrane potential.

3.2.1. Membrane potential as a function of r_p/λ_D^f, and ξ_f under different q_0

As indicated in Fig. 5, the SC model and the TMS model coincide with each other when q_0 is lower enough irrespective of the ionic valance and the value of r_p/λ_D^f. If q_0 is less than 1.0, the membrane potential can be obtained by the TMS model with simple analytical calculation instead of the SC model with cumbersome numerical calculation of the PB equation. The result can also be understood in our previous paper [1] for the explanation of the coincidence of the salt rejection and the membrane parameters by the SC model and TMS model. Moreover, Fig. 5 indicates that TMS model agrees better with SC model in the calculation of membrane potential for univalent counter-ionic salt solution than those for bivalent counter-ionic salt solution. The possible reason is that the electrostatic force between bivalent ion and membrane surface is more remarkable than that between

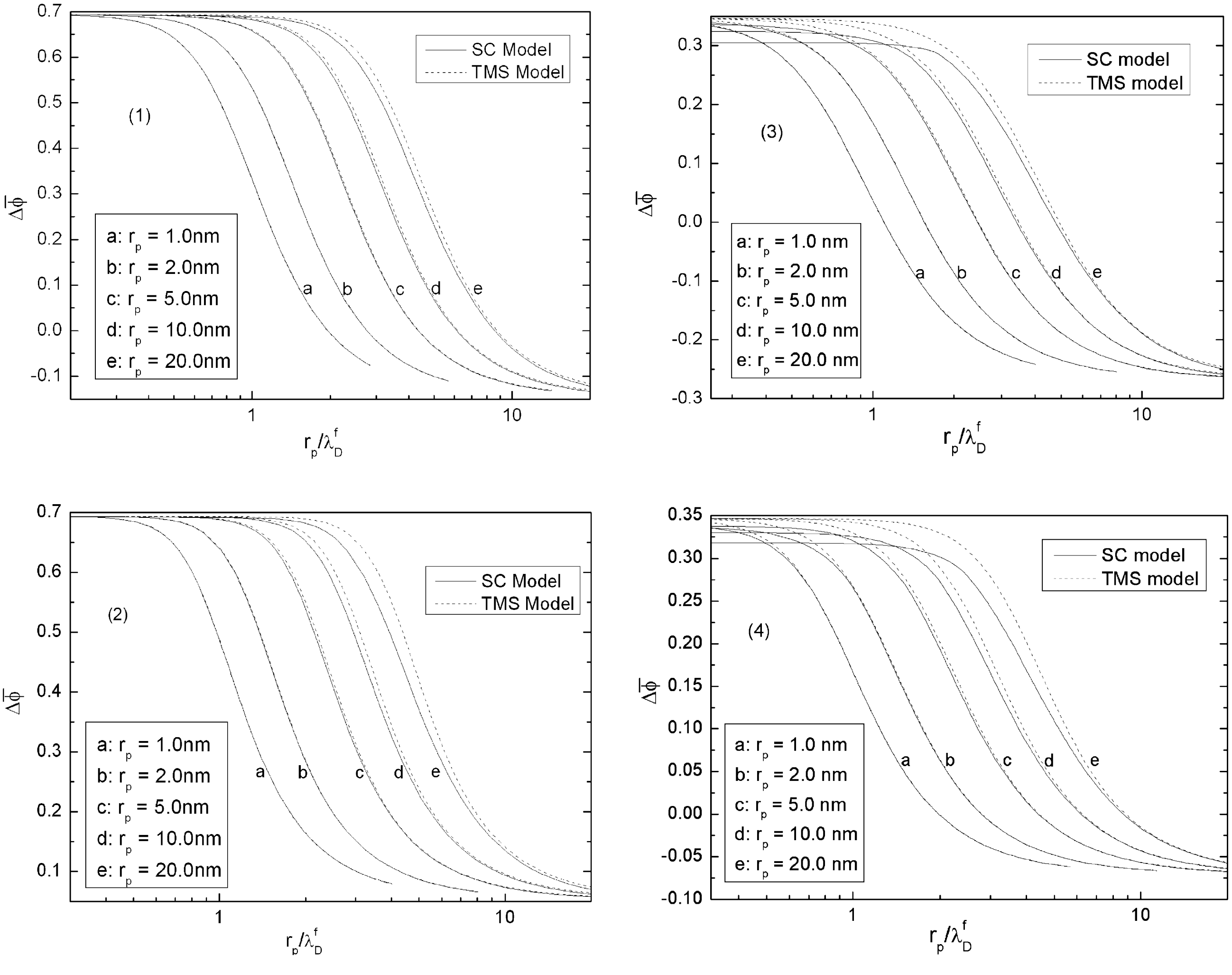

Fig. 7. $\Delta\bar{\phi}$ as a function of r_p/λ_D^f, and r_p for four electrolyte (NaCl (1); Na_2SO_4 (2); $MgCl_2$ (3); $MgSO_4$ (4)) solutions under the condition that c_f/c_p is 2.0, q_w of -6.672×10^{-3} C m^{-2}, and r_p is from 1.0 to 20.0 nm.

univalent ion and membrane surface. Another possible reason may due to the dispersal difference between bivalent ions and equivalent monovalent ions.

Basing on the relationship among ξ_f, r_p/λ_D^f and q_0, the membrane potential as a function of r_p/λ_D^f with different q_0 can be also represented as a function of ξ_f with different q_0. As illuminated in Fig. 6, $\Delta\bar{\phi}$ by the SC model shows dependence on both ξ_f and q_0. With ξ_f increasing, $\Delta\bar{\phi}$ grows monotonously and approaches ln 2.0 (the dimensionless value of Nernst potential for the concentration ratio of 2.0), while for the constant value of ξ_f, the larger q_0 is, the smaller $\Delta\bar{\phi}$ is. However, $\Delta\bar{\phi}$ by the TMS model only varies with ξ_f irrespective of q_0. The TMS model overestimates $\Delta\bar{\phi}$ as compared with the SC model. It can be explained that the partition coefficients obtain from the TMS is only related to ξ_f [9]. Basing on the expression of membrane potential (Eq. of (11)) by the TMS, one can find that $\Delta\bar{\phi}_{TMS}$ is connected with ξ_f uniquely, which is the result of neglecting the effects of the radial non-uniform ionic distribution inside pores [3]. Regarding the SC model, it assumes that the radial electrical potential and radial ion concentration obeys the Possion–Boltzmann distribution. When q_0 changes, the electrical potential, ion concentration and the coupling coefficients all change accordingly. For the case of low q_0 (q_0 less than about 1.0), $\Delta\bar{\phi}$ by the two models tend to coincide and show almost the same values irrespective of ξ_f. That is to say, if q_0 is less than 1.0, one can predict $\Delta\bar{\phi}$ by the TMS model with analytical expression instead of the SC model with cumbersome calculation of the Poision–Boltzmann equation. The same conclusion was obtained for the calculation of the salt rejection and the membrane parameters by the SC model and the TMS models [1,3].

3.2.2. Membrane potential as a function of ξ_f, and r_p/λ_D^f under different membrane radius

Fig. 7 delineate $\Delta\bar{\phi}$ as a function of r_p/λ_D^f under different r_p for four electrolyte (NaCl(1); Na_2SO_4(2); $MgCl_2$(3); $MgSO_4$ (4)) solutions at the concentration ratio c_f/c_p of 2.0, and the surface charge density q_w of -6.672×10^{-3} C m^{-2}. From the figure, the membrane potential predicted by the TMS model show good agreement with those estimated by the SC model in a low radius range irrespective of the value of r_p/λ_D^f. When r_p is less than 5.0 nm, the TMS model can completely replace the SC model in evaluating the membrane potential. The causes may be that the TMS model does not depend on the geometry [3]. The TMS model disagrees with the SC model whether the pore radius become larger.

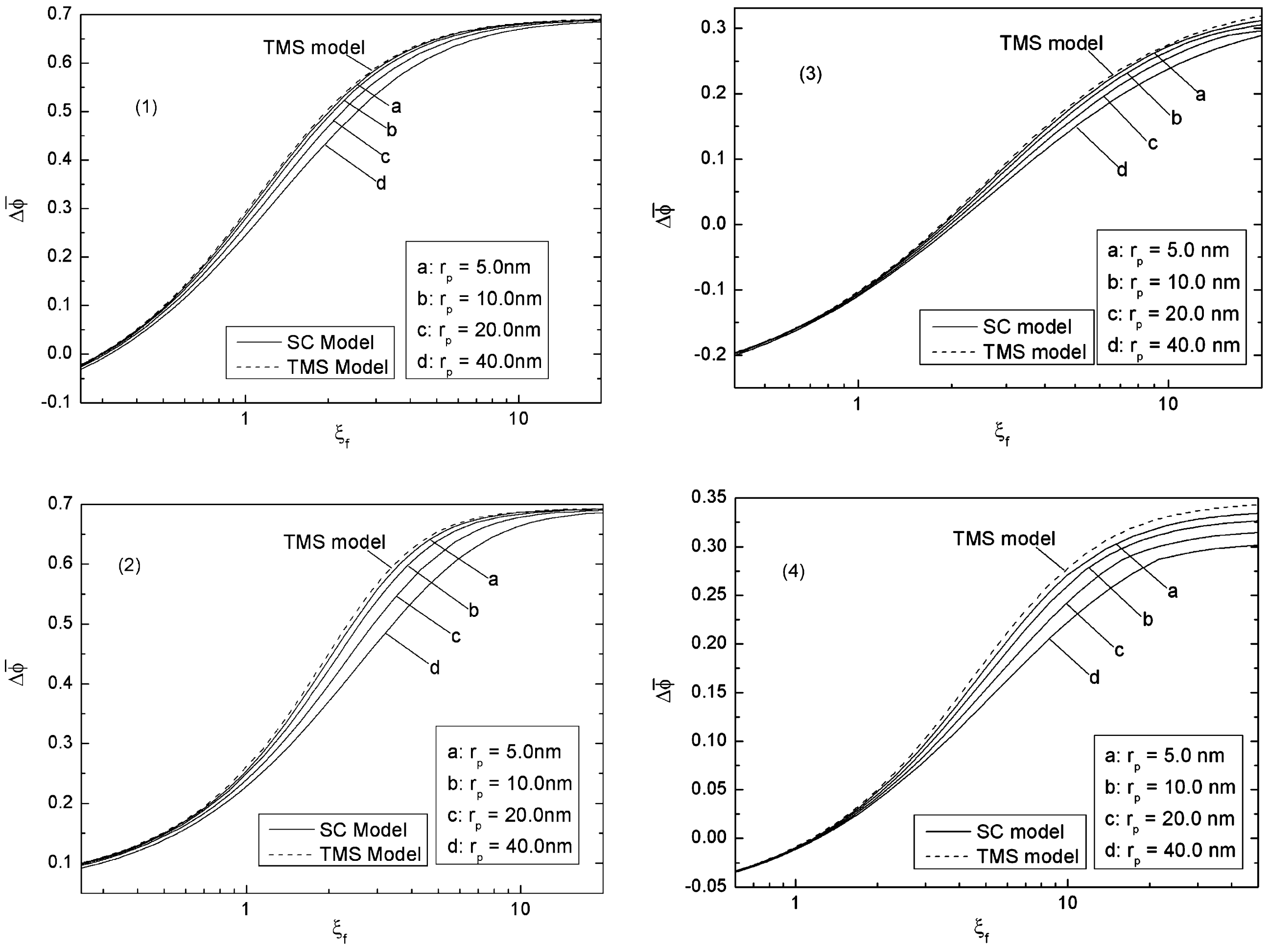

Fig. 8. $\Delta\bar{\phi}$ as a function of ξ_f, and r_p for four electrolyte (NaCl (1); Na_2SO_4 (2); $MgCl_2$ (3); $MgSO_4$ (4)) solutions under the condition that c_f/c_p is 2.0, q_w of -6.672×10^{-3} C m^{-2}, and r_p is from 1.0 to 40.0 nm.

Fig. 8 shows similar to the membrane potential as a function of two-dimensionless parameters, r_p/λ_D^f and q_0. That is, the membrane potential shows dependence on ξ_f and r_p by the SC model, but only varies with ξ_f irrespective of r_p by the TMS model. If r_p is less than 5.0 nm, the membrane potential predicted by the TMS model is consistent with those obtained by the SC model. Otherwise, the TMS model would overestimate the membrane potential. The reason is probably due to the fact that the SC model is based on the assumption of the electrical potential and ion concentration with a radial distribution in space, while the TMS model ignores the effects of the radial non-uniform ionic distribution inside pores [3]. On the other hand, it illuminates that the TMS model is independent of pore geometry, while the SC model is related with pore geometry. The similar result was obtained by examining membrane potential for a cylindrical pore and for an infinite slit pore [3].

4. Conclusions

In this present study, the TMS model, generally adopted in estimating membrane potential for 1-1 electrolyte solutions, is extended to evaluate multivalent electrolyte solutions. Through the calculation of the TMS model, the Cardano formula, introduced in the article, is favorable to calculate the Donnan equation analytically for asymmetry electrolyte (1-2, and 2-1).

On the basis of the study of different electrolyte solutions (electrovalence, concentration ration, c_f/c_p, and diffusion coefficients ratio, D_2/D_1), the following conclusion can be made. Firstly, equivalent electrolyte concentration is more suitable to characterize the membrane potential in different kinds of electrolyte solutions than electrolyte concentration. Membrane potential approaches to the Nernst potential in the low concentration region, which indicates membrane potential in monovalent cation electrolyte solution is twice as large as that in divalent cation electrolyte solution. In the high concentration region, membrane potential closes to the diffusion potential. It implies membrane potential would be reversed if the diffusion coefficient, D_2/D_1, is larger than 1.0. The reversed behavior means that the mobilities of the mobilities of counter-ion and co-ion have a crossover correspondingly, and the rejection of membrane to ions may changed from great to small, or even become minus at certain concentration region. While in the intermediate concentration region, membrane potential as a function of electrolyte concentration is almost linearity and the relationship can also be found in experiment work. The various above-mentioned anomalous phenomena can be explained expediently by the TMS model when compared with the SC model. The possible reason is that the linearized transport equations (Eqs. of (1)–(3)) are difficult to analyze due to the concentration gradient and the concentration dependence of the coupling coefficients (K_{ij}) [3] by the SC model.

From the investigation of membrane structural and electrical parameters, membrane potentials by the two models for 1-2, 2-1 and 2-2 electrolyte solutions appear to be similar to those for 1-1 electrolyte solutions reported earlier by Westermann-Clark and Christoforou [3]. The TMS model shows good agreement with the SC model in the calculation of the membrane potential when dimensionless surface charge density, q_0, is less than 1.0, and the radius, r_p, is less than 5.0 nm. Otherwise, the TMS model would overestimate the membrane potential. Furthermore, the membrane potential shows dependence on the ratio of the volume charge density to equivalent electrolyte concentration, ξ_f and q_0/r_p by the SC model, but only varies with ξ_f irrespective of q_0/r_p by the TMS model. The reason is probably due to the fact that the SC model considers the radial of the electrical potential and ion concentration in space, while the TMS model ignores the effects of the radial non-uniform ionic distribution inside pores [3].

In view of the theoretical results presented above, it seems the TMS model is favorable to calculate the membrane potential of charged porous membrane and explain the various correlative phenomena in many physical situations.

Acknowledgements

The work is supported financially by National Basic Research Program of China (2003CB615701) and National Natural Science Foundation of China (20376040).

Nomenclature

c	concentration in external solution or in capillary of membrane (mol m^{-3})
D_i	diffusion coefficient of ion i (m^2 s^{-1})
D_S	generalized diffusivity defined in Eq. (3.42) (m^2 s^{-1})
F	Faraday constant (=96,487 C mol^{-1})
I	current density (A m^{-2})
I^*	dimensionless current density
j	ion flux in axial direction of capillary (mol m^{-2} s^{-1})
J_S	average value of ion flux in capillary (mol m^{-2} s^{-1})
J_S^*	dimensionless average value of ion flux
J_V	volumetric flux in capillary (m s^{-1})
k_i	local distribution coefficient of ion i ($i = 1, 2$)
$\bar{k}_i$	averaged distribution coefficient of ion i ($i = 1, 2$)
K_{ij}	defined in Appendix A
L_i	defined in Appendix B
L_{ij}	phenomenological coefficients defined in Appendix B of Part I
L_p	pure water permeability of capillary (m^3 m^{-2} s^{-1} pa^{-1})
P	hydraulic pressure (Pa)
P_0	effective pressure in capillary ($P_0 = P - RT(\nu_1 + \nu_2)c$) (Pa)
ΔP	difference of hydraulic pressure in capillary (Pa)
Pe	Peclet number
Pe_m	generalized Peclet number $Pe_m = J_V \Delta x / D_S = Pe(D_1/D_S)$

q_w	the surface charge density of capillary ($C\,m^{-2}$)
q_0	dimensionless potential gradient on the capillary wall
r	radial variable of capillary (m)
r_p	radius of capillary (m)
R	rejection
R_g	or gas constant ($8.314\,J\,mol^{-1}\,K^{-1}$)
ts	ionic mobility
T	temperature (K)
u	ionic mobility ($mol\,m^2\,J^{-1}\,s^{-1}$)
u_x	mass flux in axial direction of capillary ($m\,s^{-1}$)
u_x^*	dimensionless mass flux in axial direction
U_m	average value of mass flux in capillary ($m\,s^{-1}$)
x	axial variable of capillary (m)
Δx	length of capillary (m)
X	charge density based on volume of capillary ($mol\,m^{-3}$)
z	electrochemical valence of ion
Greek letters	
ε_r	relative dielectric constants of aqueous electrolyte solution (78.303)
ε_0	dielectric constants of vacuum ($8.8542 \times 10^{-12}\,C^2\,J^{-1}\,m^{-1}$)
λ	ratio of Debye length of electrolyte to pore radius
λ_D	Debye length of electrolyte solution (m)
μ	viscosity of electrolyte solution (Pa s)
ν_i	stoichiometric coefficient of electrolyte
ξ	ratio of volume charge density in membrane to electrolyte concentration
π	osmotic pressure in capillary defined as $RT(\nu_1+\nu_2)c$ (Pa)
ρ_c	excess charge density of electrolyte in capillary ($C\,m^{-3}$)
σ	reflection coefficient
Φ	total electrostatic potential inside capillary (V)
ϕ	electrostatic potential divided in axial direction (V)
ψ	electrostatic potential divided in radial direction (V)
ω	solute permeability coefficient ($mol\,m^2\,J^{-1}\,s^{-1}$)
Subscripts	
b	bulk solution
i	ith ion ($i=1$: counterion; $i=2$: co-ion)
p	permeate
s	solute
Superscripts	
D	Donnan equilibrium
m	membrane phase
–	dimensionless factor

References

[1] X.L. Wang, T. Tsuru, S. Nakao, S. Kimura, Electrolyte transport through nanofiltration membranes by space-charge model and the comparison with Teorell–Meyer–Sievers model, J. Membr. Sci. 103 (1995) 117–133.

[2] Y. Kobatake, Irreversible electrochemical processes of membranes, J. Chem. Phys. 28 (1958) 146–153.

[3] G.B. Westermann-Clark, C.C. Christoforou, The exclusion–diffusion potential in charged porous membranes, J. Electroanal. Chem. 198 (1986) 213–231.

[4] Y. Kobatake, N. Takeguchi, Y. Toyoshima, H. Fujita, Studies of membrane phenomena. I. Membrane potential, J. Phys. Chem. 69 (1965) 3981–3988.

[5] Y. Toyoshima, Y. Kobatake, H. Fujita, Studies of membrane potential. Part 4. Membrane potential and permeability, Trans. Faraday Soc. 63 (1967) 2814–2827.

[6] G.J. Hills, P.W.M. Jacobs, N. Lakshminarayanaiah, Membrane potentials I. the theory of the e.m.f. of cells containing ion-exchange membranes, Proc. Roy. Soc. (London) A262 (1961), 246–256, 257–270.

[7] N. Lakshminarayanaiah, Transport Phenomena in Membranes, Academic Press, New York, 1966.

[8] V.V. Nikonenko, K.A. Lebedev, V.I. Zabolotsky, L. Dammak, C. Larchet, B. Auclair, A mathematical model for the bi-ionic potential, Eur. Polym. J. 33 (7) (1997) 1057–1059.

[9] X. Lefebvre, J. Palmeri, P. David, Nanofiltration theory: an analytic approach for single salts, J. Phys. Chem. B 108 (43) (2004) 16811–16824.

[10] F.A. Morrison Jr., J.F. Osterle, Electrokinetic energy conversion in ultrafine capillaries, J. Chem. Phys. 43 (6) (1965) 2111–2114.

[11] R.J. Gross, J.F. Osterle, Membrane transport characteristics of ultrafine capillaries, J. Chem. Phys. 49 (1) (1968) 228–233.

[12] J.C. Fair, J.F. Osterle, Reverse electrodialysis in charged capillary membranes, J. Chem. Phys. 54 (8) (1971) 3307–3316.

[13] V. Sasidhar, E. Ruckenstein, Anomalous effects during electrolyte osmosis across charged porous membranes, J. Colloid Interf. Sci. 85 (2) (1982) 332–362.

[14] G.B. Westermann-Clerk, J.L. Anderson, Experimental verification of the space-charge model for electrokinetics in charged microporous membranes, J. Electrochem. Soc. 130 (4) (1983) 839–847.

[15] C.C. Christoforou, G.B. Westermann-Clerk, J.L. Anderson, The streaming potential and inadequacies of the Helmholtz equation, J. Colloid Interf. Sci. 106 (1) (1985) 1–11.

[16] J.R. Philip, R.A. Wooding, Solution of the Poisson–Boltzmann equation about a cyclindrical particle, J. Chem. Phys. 52 (2) (1970) 953–959.

[17] S. Levine, J.R. Marriott, G. Neale, N. Epstein, Theory of electrokinetic flow in fine cylindrical capillaries at high zeta-potentials, J. Colloid Interf. Sci. 52 (1) (1975) 136–149.

[18] L. Martinez, M.A. Gigosos, A. Hernandez, F. Tejerina, Study of some electrokinetic phenomena in charged microapillary porous membranes, J. Colloid Interf. Sci. 35 (1987) 1–20.

[19] P. Rievet, A. Szymczyk, C. Labbez, B. Aoubiza, C. Simon, A. Foissy, J. Pagetti, Determining the zeta potential of porous membranes using electrolyte conductivity inside pores, J. Colloid Sci. 235 (2001) 383–390.

[20] C. Labbez, P. Rievet, A. Szymczyk, B. Aoubiza, A. Vidonne, J. Pagetti, Theoretical study of the electrokinetic and electrochemical behaviors of two-layer composite membranes, J. Colloid Sci. 184 (2001) 79–85.

[21] P. Rievet, A. Szymczyk, B. Aoubiza, J. Pagetti, Evalution of three methods for the characterization of the membrane-solution interface: streaming potential, membrane potential and electrolyte conductivity inside pores, J. Colloid Sci. 168 (2000) 87–100.

[22] H.J.M. Hijnen, J. Van, J.A.M. Smit, The application of the space-charge model to the permeability properties of charged microporous membranes, J. Colloid Interf. Sci. 107 (2) (1985) 525–539.

[23] J.A.M. Smit, Reverse osmosis in charged membranes: Analytical predictions from the space-charge model, J. Colloid Interf. Sci. 132 (2) (1989) 413–424.

[24] V. Sasidhar, E. Ruckenstein, Electrolyte osmosis through capillaries, J. Colloid Interf. Sci. 82 (2) (1981) 439–457.

[25] P. Neogi, E. Ruckenstein, Viscoelectric effects in reverse osmosis, J. Colloid Interf. Sci. 79 (1) (1981) 159–169.

[26] T. Teorell, Diffusion effect upon ionic distribution. I. Theoretical, P. Natl. Acad. Sci. U.S.A. 21 (15) (1935) 152–161.

[27] K.H. Sievers, J.F. Sievers, Helv. Chim. Acta 19 (1936), 649–664, 665–677, 987–995.

[28] E. Hoffer, O. Kedem, Ion separation by hyperfiltration through charged membranes. I. Calculation based on TMS model, Ind. Eng. Chem. Process Des. Develop. 11 (2) (1972) 221–225.

[29] T. Tsuru, S.I. Nakao, S. Kimura, Calculation of ion rejection by extended Nernst–Planck equation with charged reverse osmosis membranes for single and mixed electrolyte solutions, J. Chem. Eng. Jpn. 24 (4) (1991) 511–517.

[30] J.M.M. Peeters, J.P. Boom, M.H.V. Mulder, H. Strathmann, Retention measurements of nanofiltration membranes with electrolyte solutions, J. Membr. Sci. 145 (1998) 199–209.

[31] J.S. Zhou, R.F. Childs, A.M. Mika, Calculation of the salt separation by negatively charged gel-filled membranes, J. Membr. Sci. 260 (2005) 164–173.

[32] J.G. Aleman, J.M. Dickson, Mathematical modeling of nanofiltration membranes with mixed electrolyte solutions, J. Membr. Sci. 235 (2004) 1–13.

[33] X. Lefebvre, J. Palmeri, Nanofiltration theory: good co-ion exclusion approximation for single salts, J. Phys. Chem. B. 109 (12) (2005) 5525–5540.

[34] X.L. Wang, Model calculation and experimental investigation on electrokinetic properties of charged porous membranes, Abstracts Orals, in: ICOM’2005, Seoul: August 21–28, 2005.

[35] T.W. Xu, Y.Q. Fu, X.L. Wang, Membrane potential model for an asymmetrical nanofiltration membrane-consideration of non-continuous concentration at the interface, Desalination 171 (2) (2005) 155–165.

[36] J. Palmeri, P. Blanc, A. Larbot, P. David, Theory of pressure-driven transport of neutral solutes and ios in porous ceramic nanofiltration membranes, J. Membr. Sci. 160 (1999) 141–170.

[37] X.F. Xing, Investigation on solutions of cubic equations with one unkown, J. Central Univ. Nation. (Nat. Sci. Ed.) 12 (3) (2003) 207–218.

[38] J. Benavente, G. Jonsson, Effect of adsorption of charged macromolecules on streaming and membrane potential values measured with a microporous polysulfone membrane, Sep. Sci. Technol. 32 (10) (1997) 1699–1710.

[39] A. Cañas, J. Benavente, Electrochemical characterization of an asymmetric nanofiltration membrane with NaCl and KCl solutions: influence of membrane asymmetry on transport parameters, J. Colloid Interf. Sci. 246 (2) (2002) 328–334.